Exploration of Matrix Effects in Laser Ablation Inductively Coupled Plasma Mass Spectrometry Imaging of Cisplatin Treated Tumours

Calum J. Greenhalgh,† Ellie Karekla,‡ Gareth J. Miles,‡ Ian R. Powley,‡ Catia Costa,ǂ Janella de Jesus,‖ Melanie J. Bailey,‖ Catrin Pritchard,‡ Marion MacFarlane,§ J. Howard Pringle‡ and Amy J. Managh†*

† Department of Chemistry, Loughborough University, Loughborough, Leicestershire, LE11 3TU. UK E-mail: A.J.Managh@lboro.ac.uk

‡ Leicester Cancer Research Centre, University of Leicester, Robert Kilpatrick Building, Leicester Royal Infirmary, Leicester, LE2 7LX, UK.

ǂ Ion Beam Centre, University of Surrey, Guildford, GU2 7XH, UK.

‖ Department of Chemistry, University of Surrey, Guildford, GU2 7XH, UK.

§ MRC Toxicology Unit, University of Cambridge, Hodgkin Building, Leicester, LE1 9HN, UK.

Electronic Supporting Information

Table of Contents

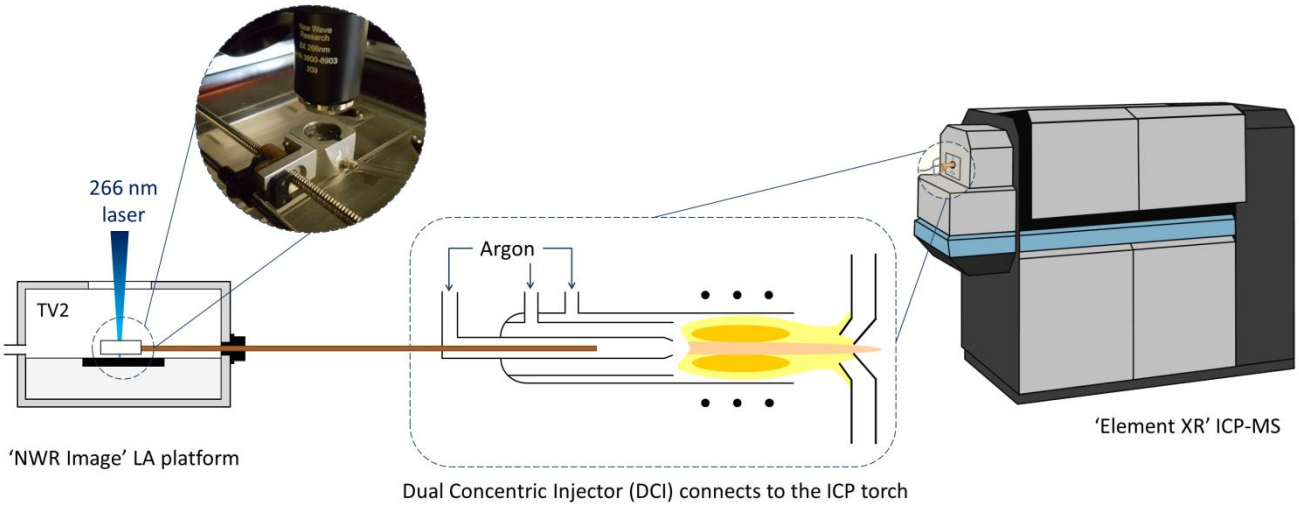

Figure S1. Schematic overview of the LA-ICP-MS instrumentation. A low-dispersion ablation cell was used within the TwoVol2 chamber, in conjunction with a Dual Concentric Injector. This maintained a constant diameter conduit (shown in brown) from point of ablation into the ICP. This reduces turbulent mixing of the aerosol during transport and is hypothesised to keep material on axis with the orifice in the cones, to provide an increase in sensitivity.

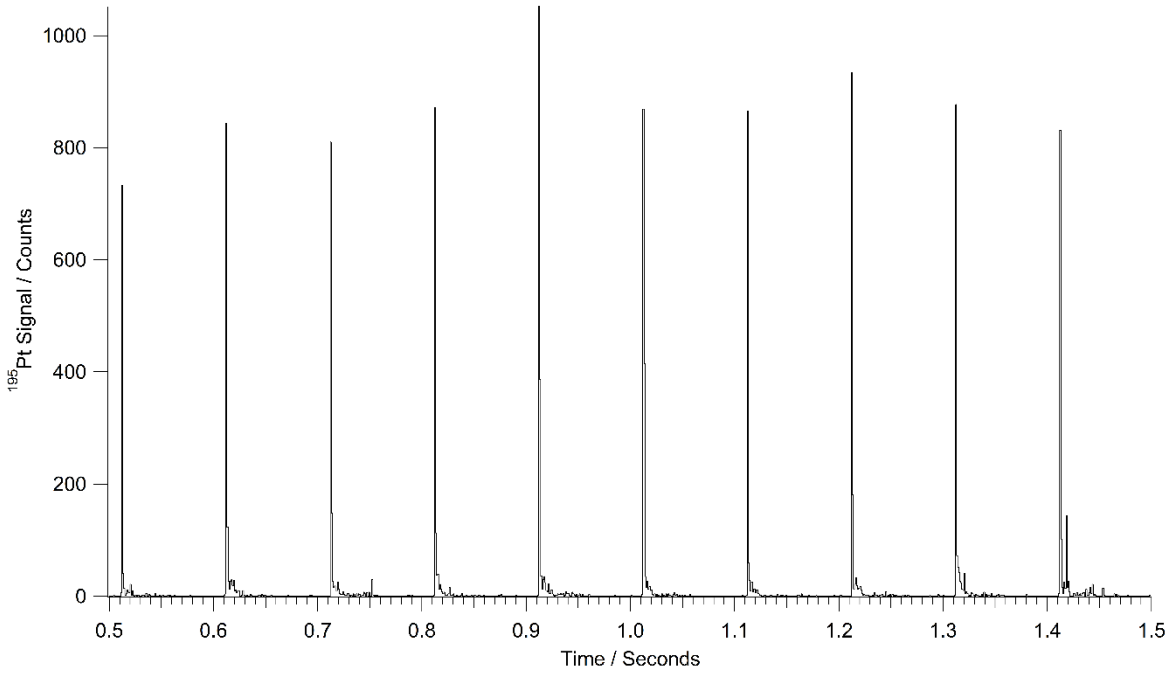

Figure S2. Representative pulse response time from the ablation of gelatine spiked with 50 µg/mL platinum using a 2 µm spot and 10 Hz repetition frequency. Data points are spaced at 1 ms intervals.

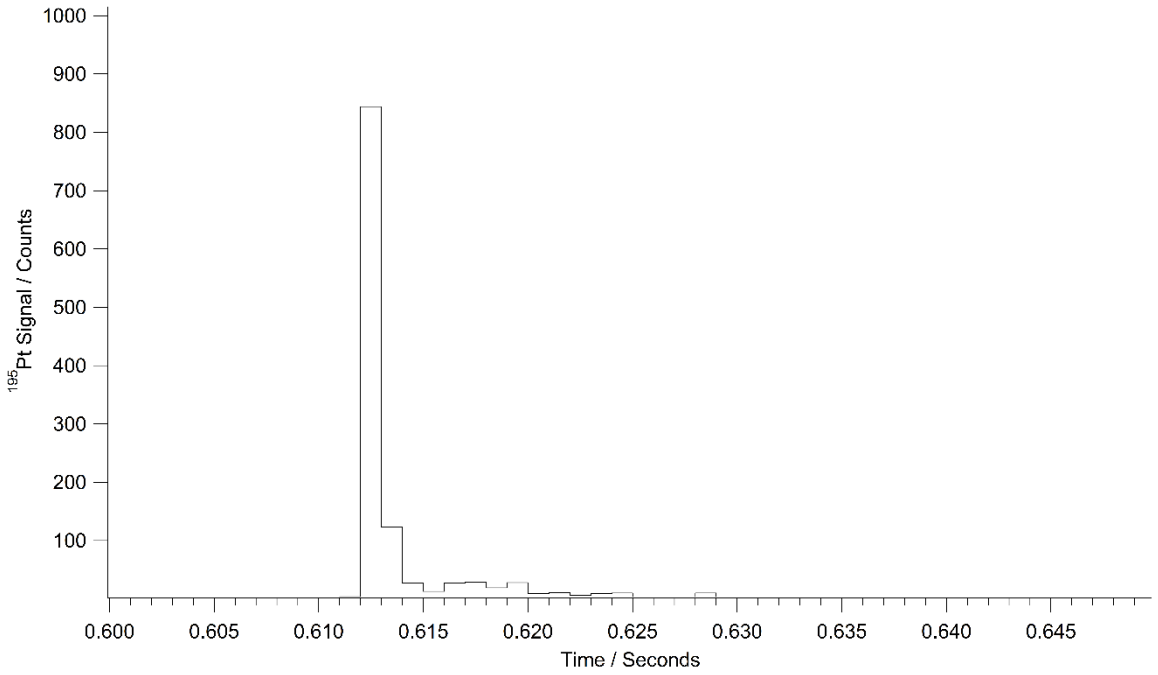

Figure S3. Isolated view of the pulse response time from peak 2 in figure S2, demonstrating that peak width at 10% peak height is achieved in less than 10 ms at FW0.1M. Data points are spaced at 1 ms intervals.

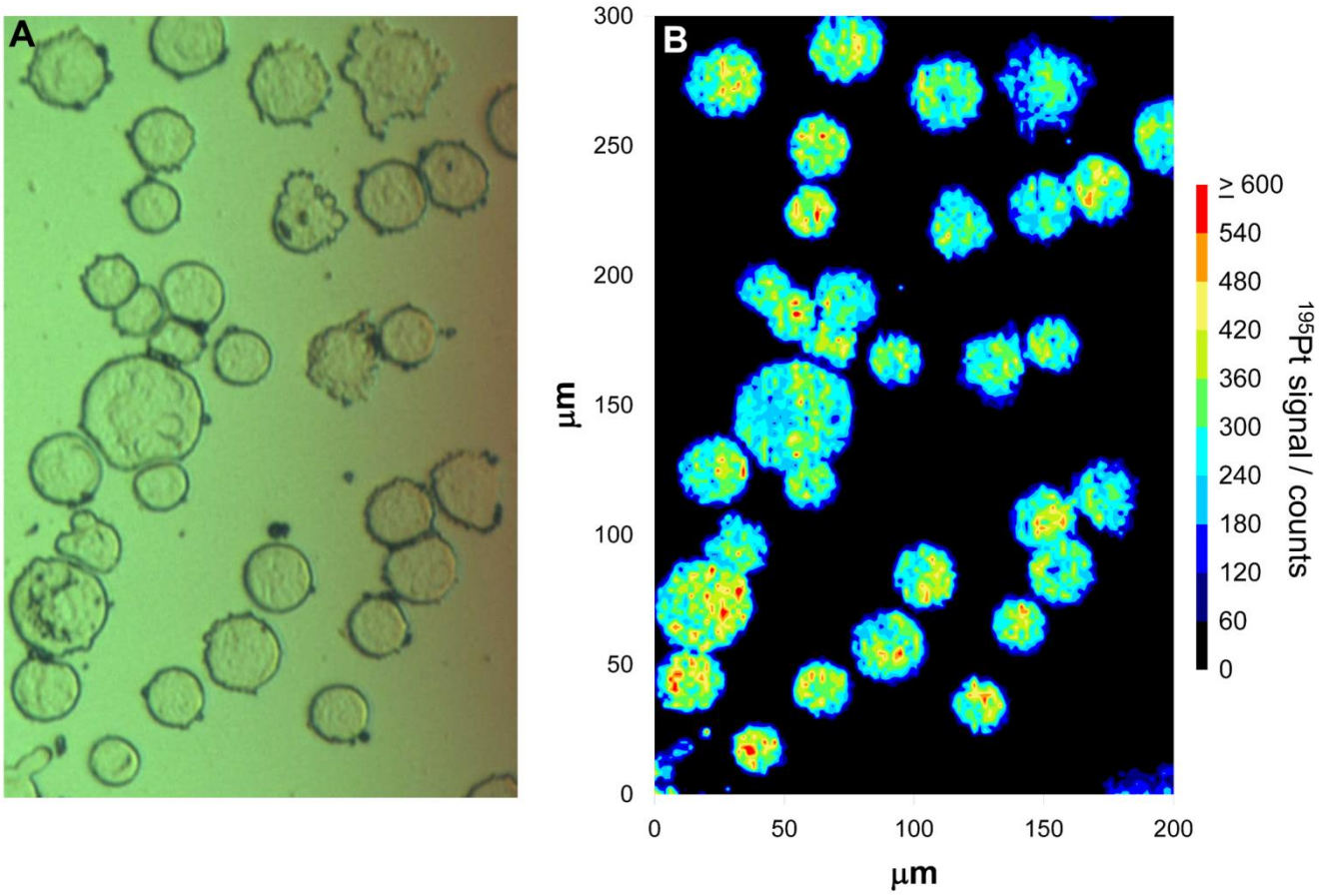

Figure S4. Optimisation experiment showing the analysis of cultured cells. A549 cells were labelled *in vitro* with 100 µM cisplatin and placed onto slides using cytocentrifugation. Image A is a microscopic image of the cultured cells, with the corresponding LA-ICP-MS analysis of Pt distribution shown in image B. Individual cells can be distinguished using a 2 µm spot size.

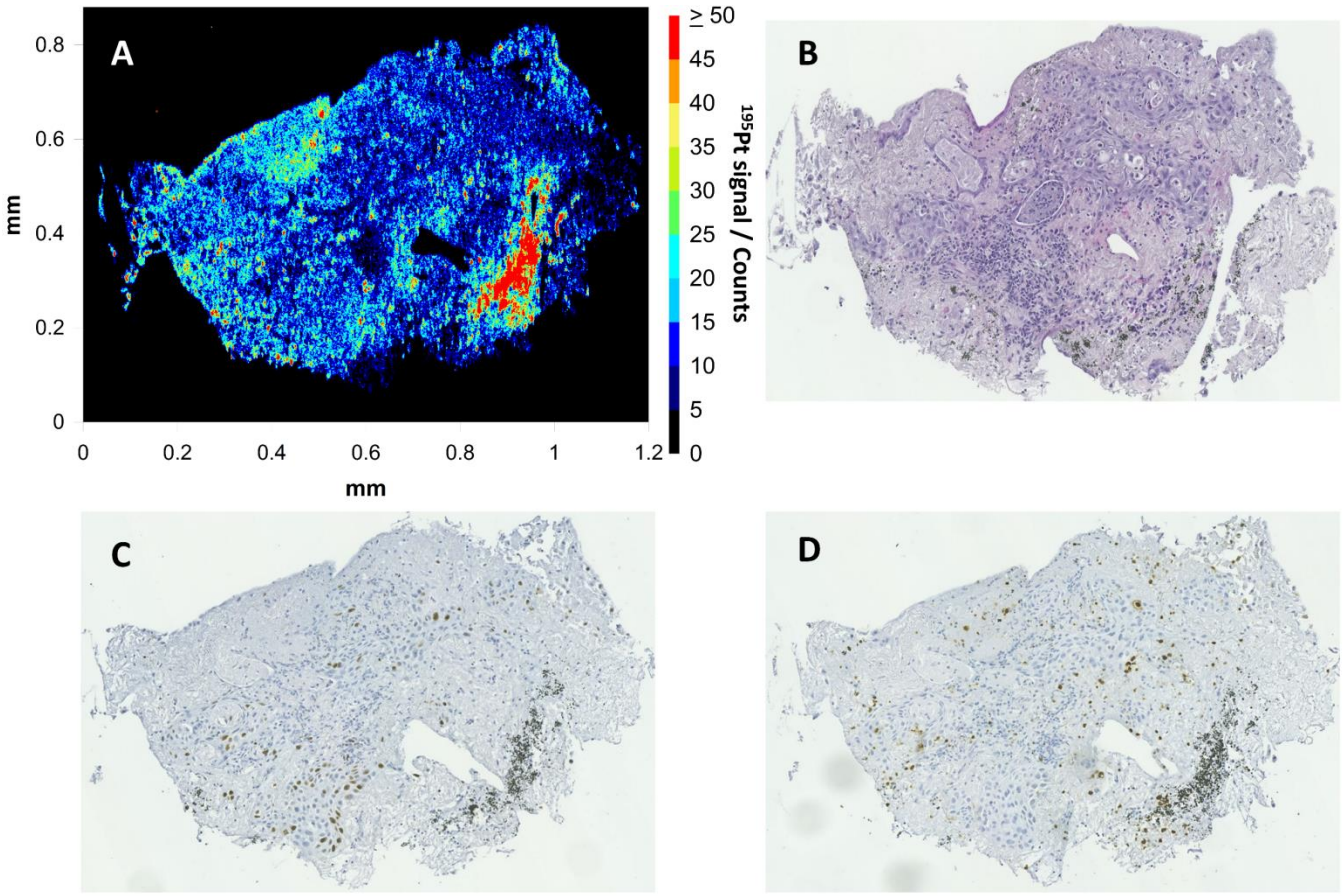

Figure S5. Explant dosed with 1 µM cisplatin from a case showing dose dependent resistance. Image A displays the Pt signal from LA-ICP-MS imaging. B displays H&E staining of a consecutive section, while C and D display Ki67 and cPARP immunohistochemistry respectively.

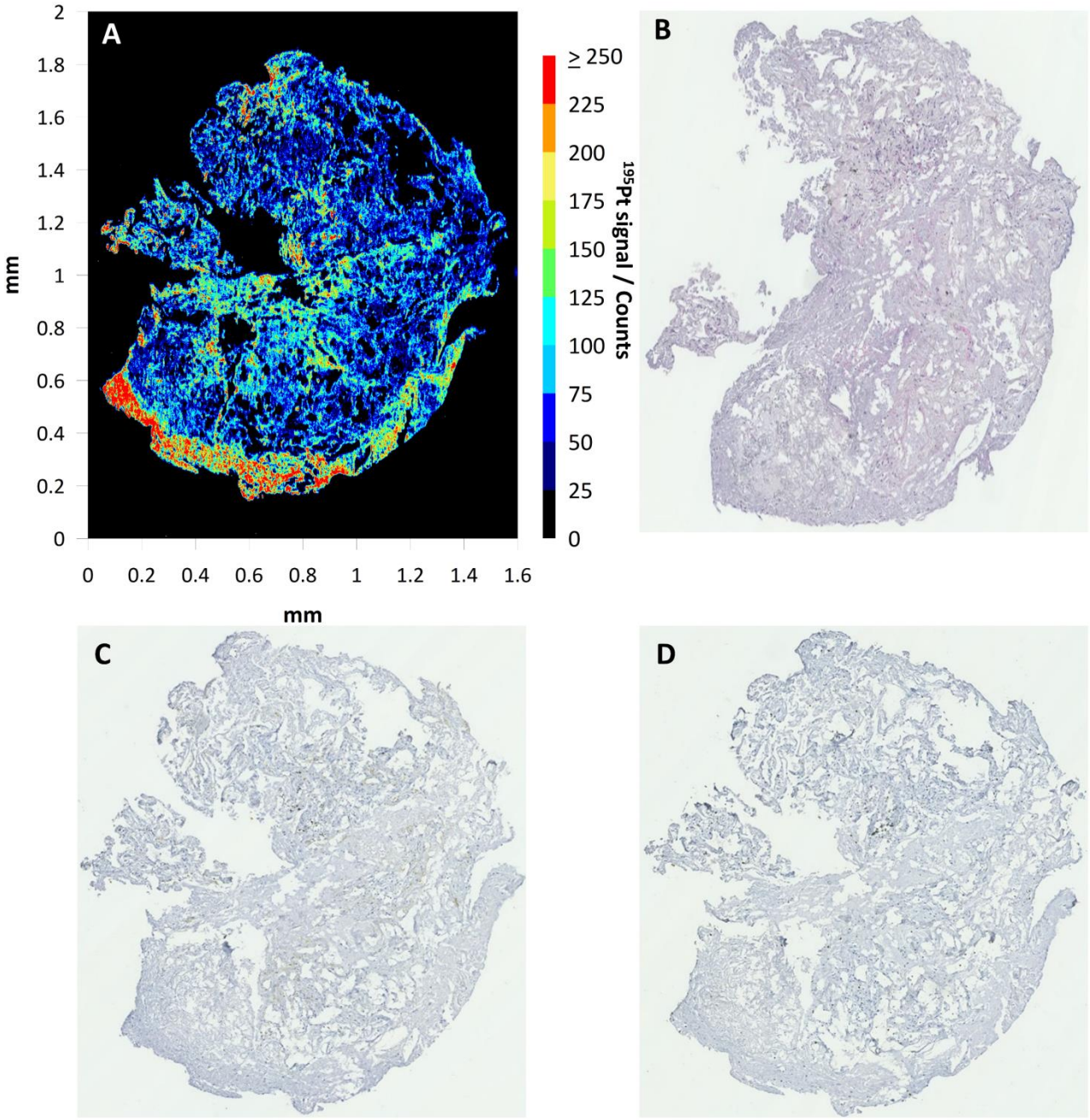

Figure S6. Explant dosed with 10µM cisplatin from a case showing dose dependent resistance. Image A displays the Pt signal from LA-ICP-MS imaging. B displays H&E staining of a consecutive section, while C and D display Ki67 and cPARP immunohistochemistry respectively.

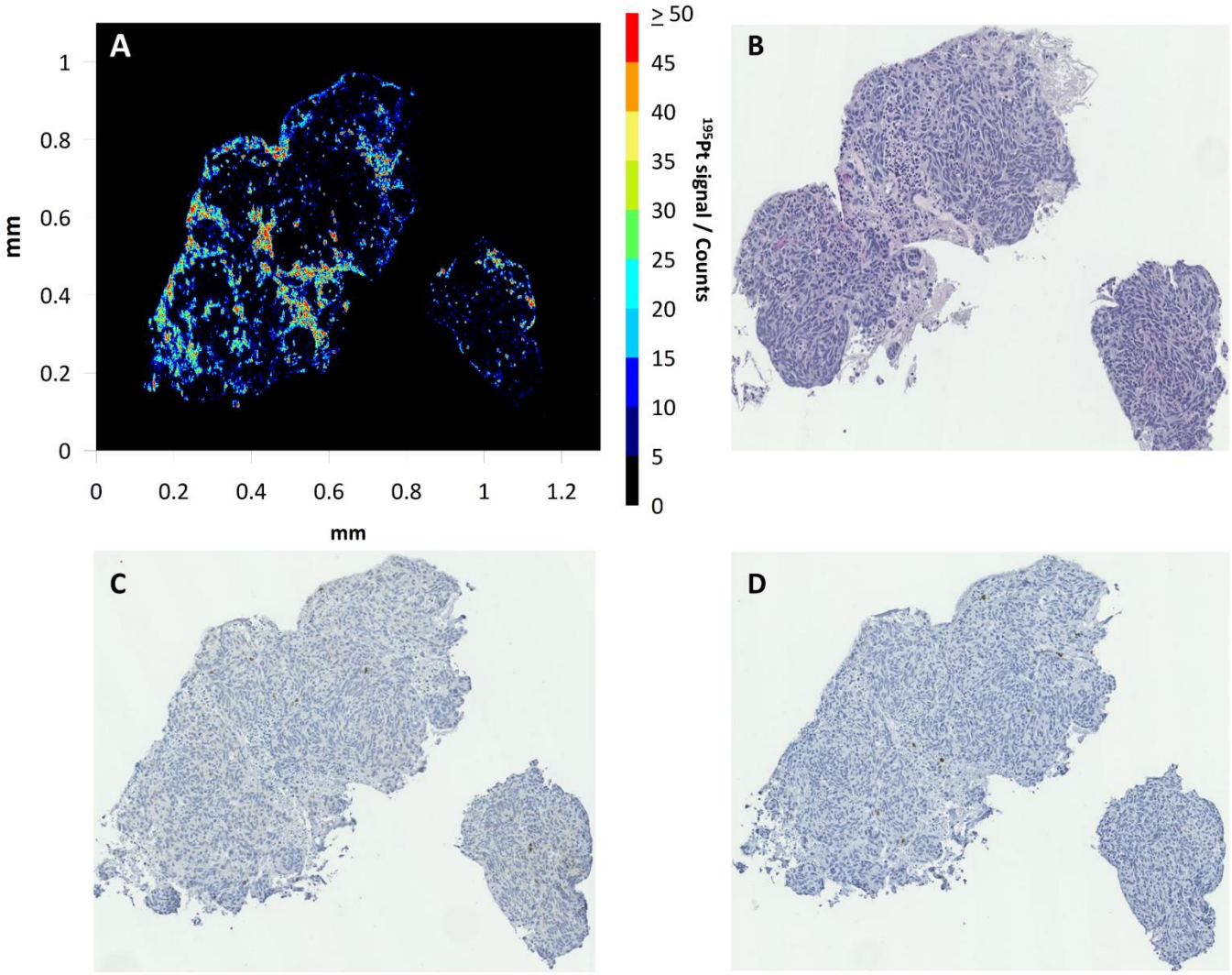

Figure S7. Cisplatin resistant explant dosed with 1µM cisplatin. Image A displays the Pt signal from LA-ICP-MS imaging. B displays H&E staining of a consecutive section, while C and D display Ki67 and cPARP immunohistochemistry respectively.

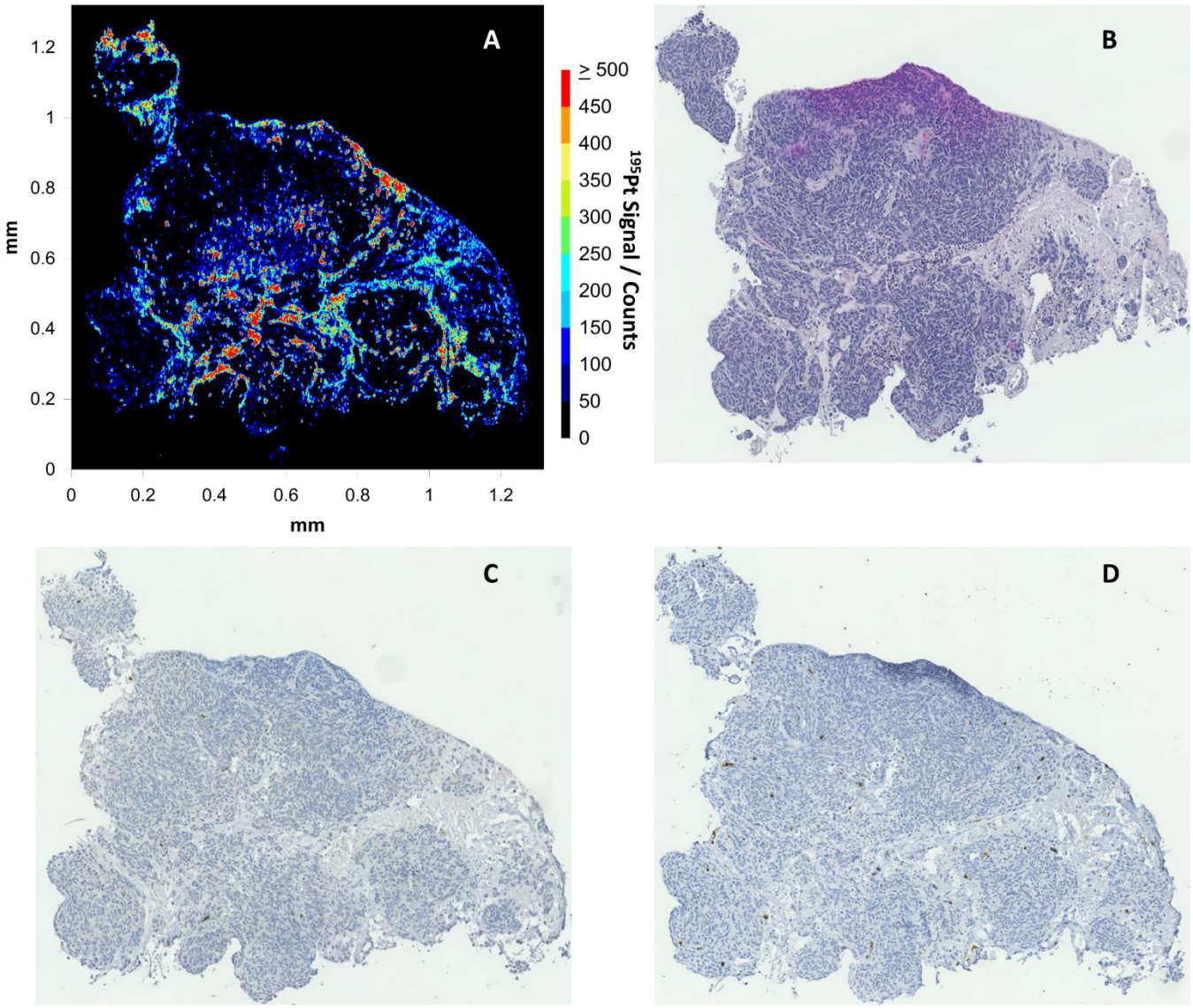

Figure S8. Cisplatin resistant explant dosed with 10µM cisplatin. Image A displays the Pt signal from LA-ICP-MS imaging. B displays H&E staining of a consecutive section, while C and D display Ki67 and cPARP immunohistochemistry respectively.

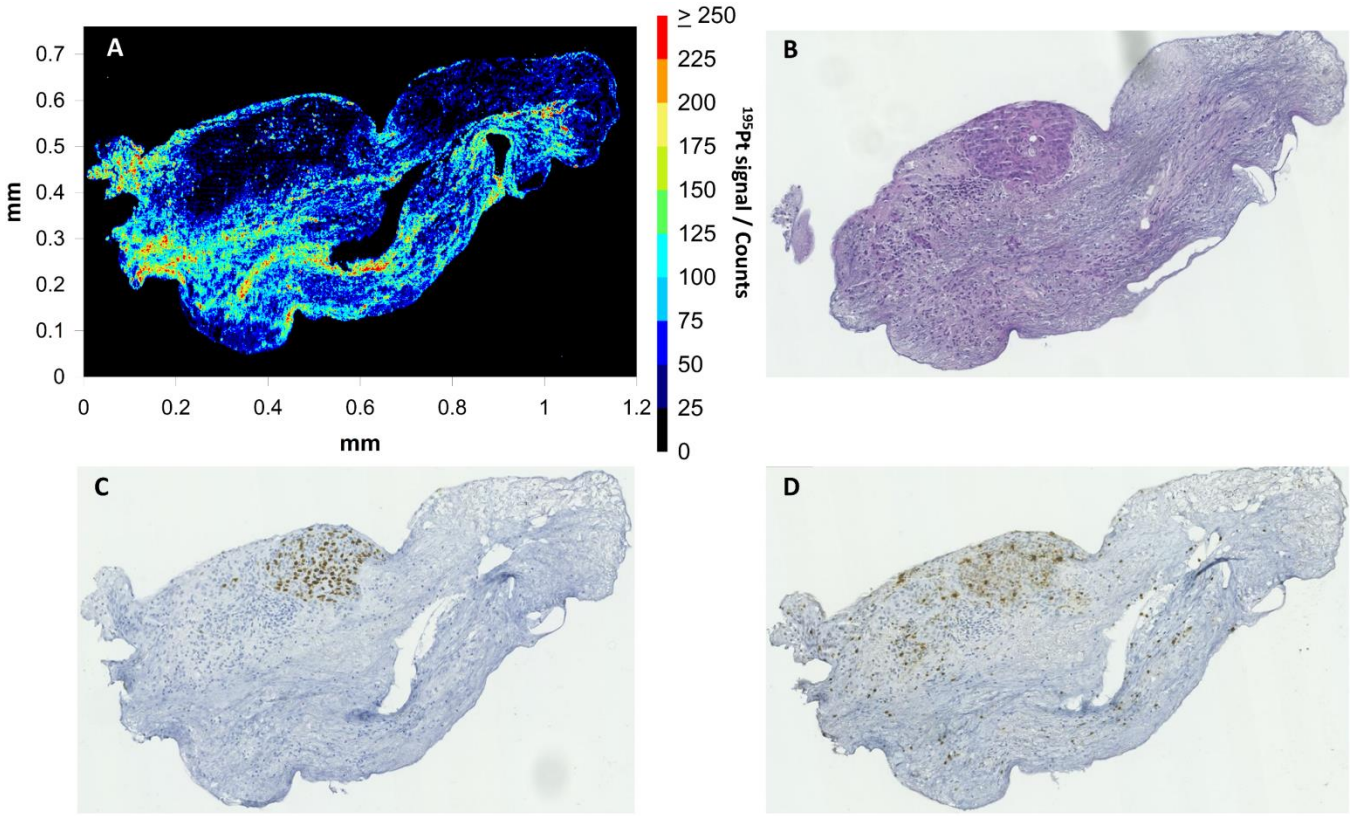

Figure S9. Cisplatin sensitive explant dosed with 1µM cisplatin. Image A displays the Pt signal from LA-ICP-MS imaging. B displays H&E staining of a consecutive section, while C and D display Ki67 and cPARP immunohistochemistry respectively.

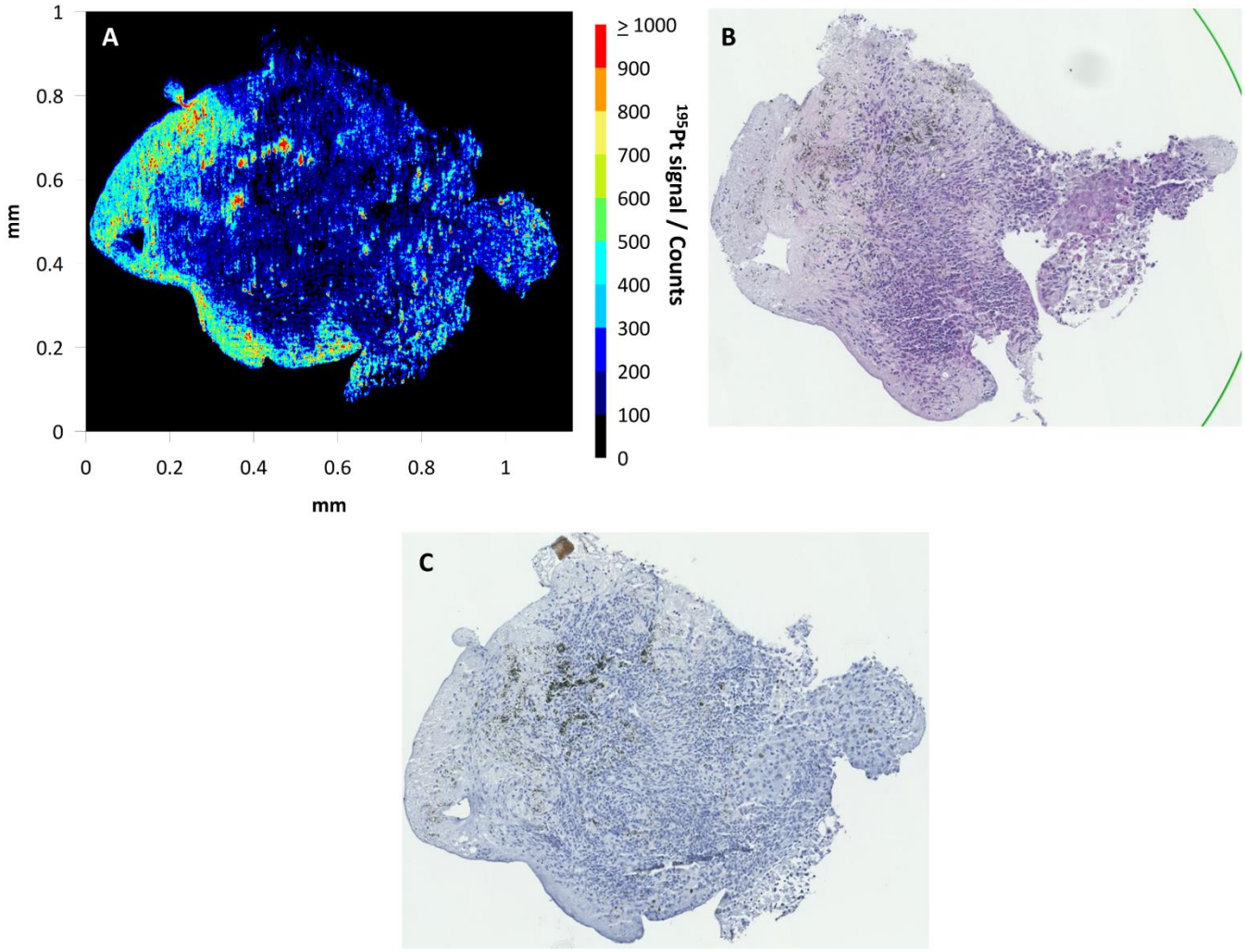

Figure S10. Cisplatin sensitive explant dosed with 10µM cisplatin. Image A displays the Pt signal from LA-ICP-MS imaging. B displays H&E staining of a consecutive section, while C displays Ki67 immunohistochemistry. There was no cPARP image available for this section.

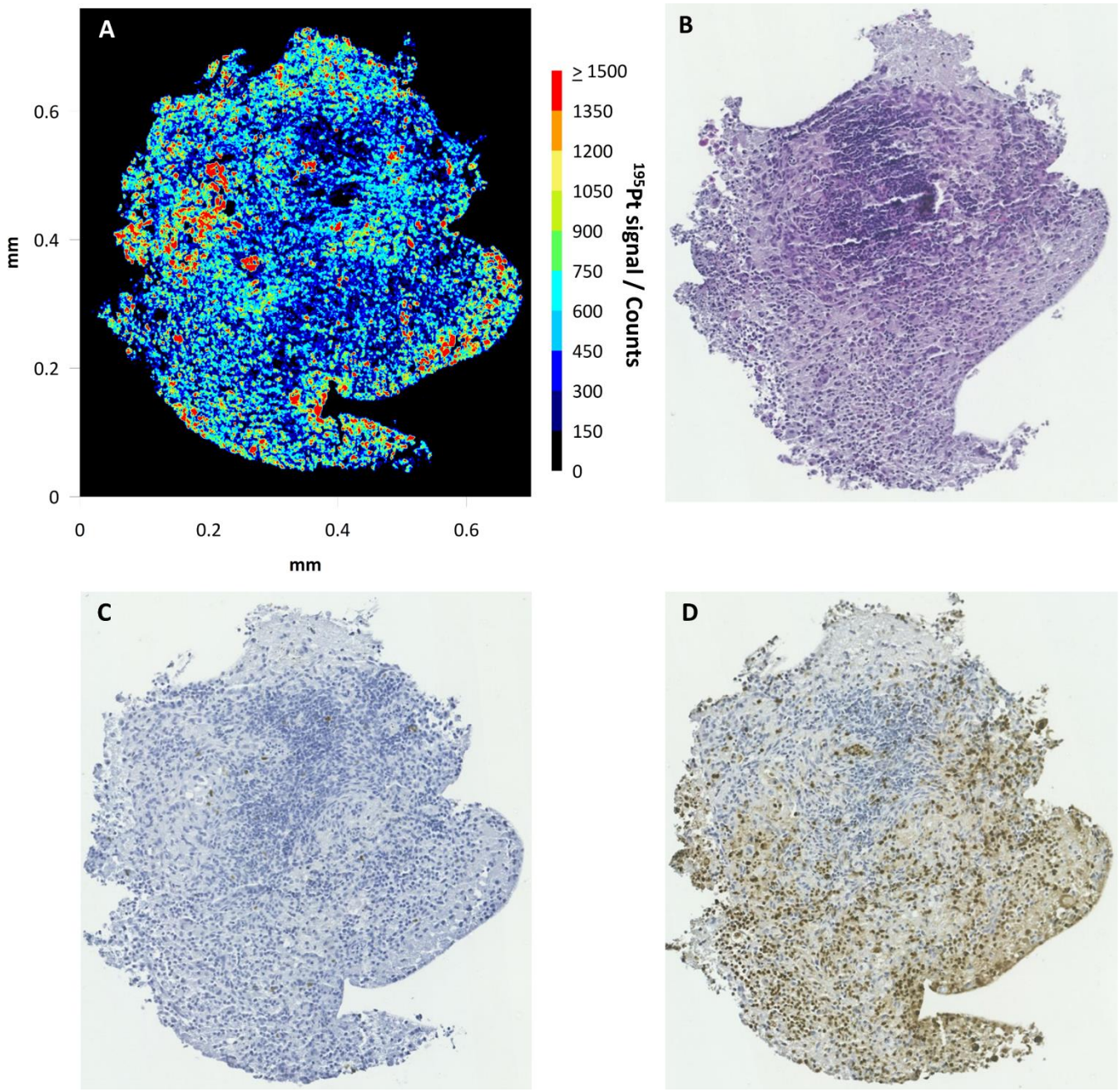

Figure S11. Cisplatin sensitive explant dosed with 50µM cisplatin. Image A displays the Pt signal from LA-ICP-MS imaging. B displays H&E staining of a consecutive section, while C and D display Ki67 and cPARP immunohistochemistry respectively.

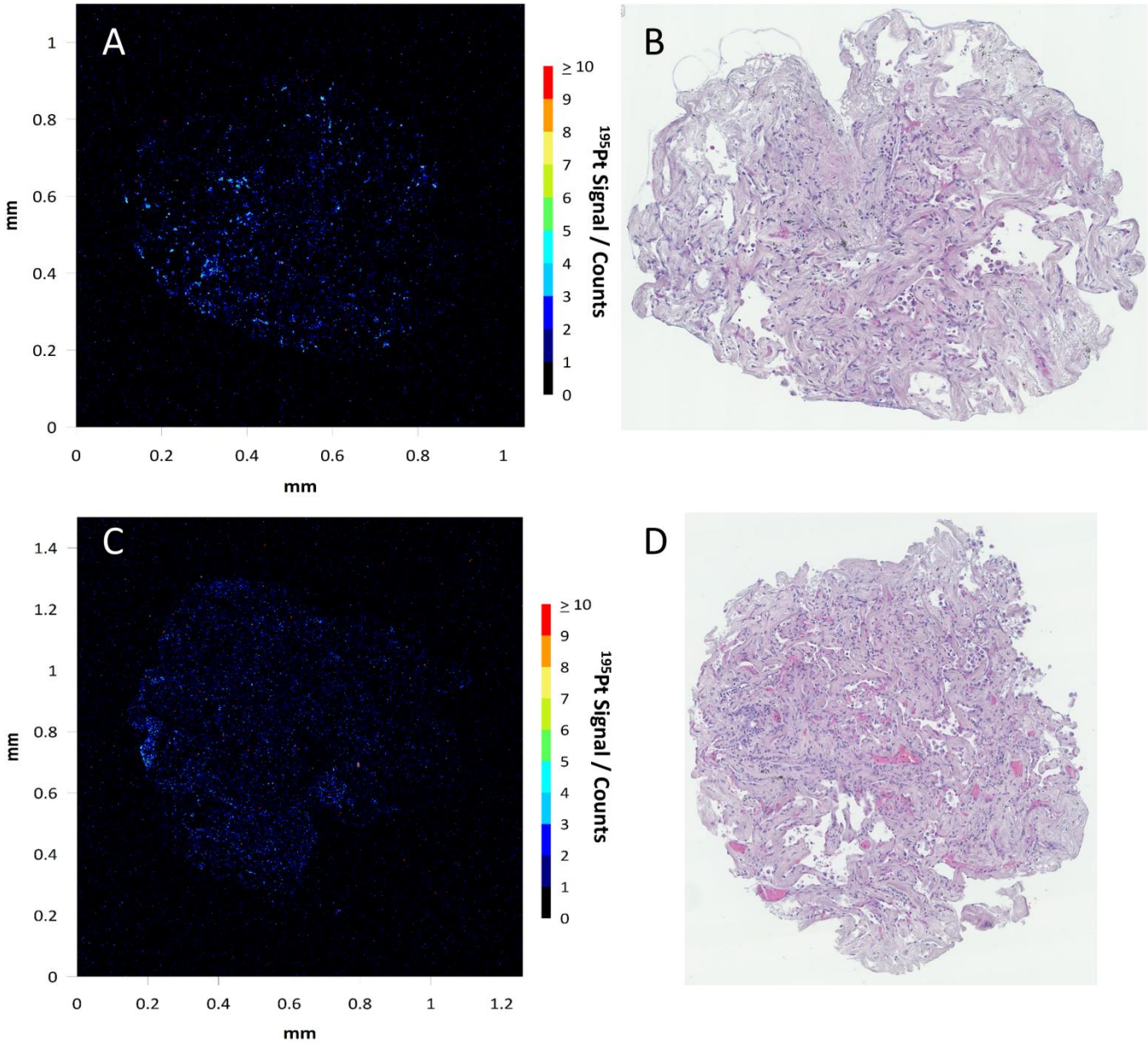

Figure S12. Analysis of Platinum in non-Pt dosed explant controls. Image A displays the Pt signal from LA-ICP-MS imaging in a control section containing carbon deposits, with the corresponding H&E stained consecutive section shown in B. Image C displays the Pt signal from LA-ICP-MS imaging in a second control section, without visible carbon deposits, with the corresponding H&E stained consecutive section shown in D.

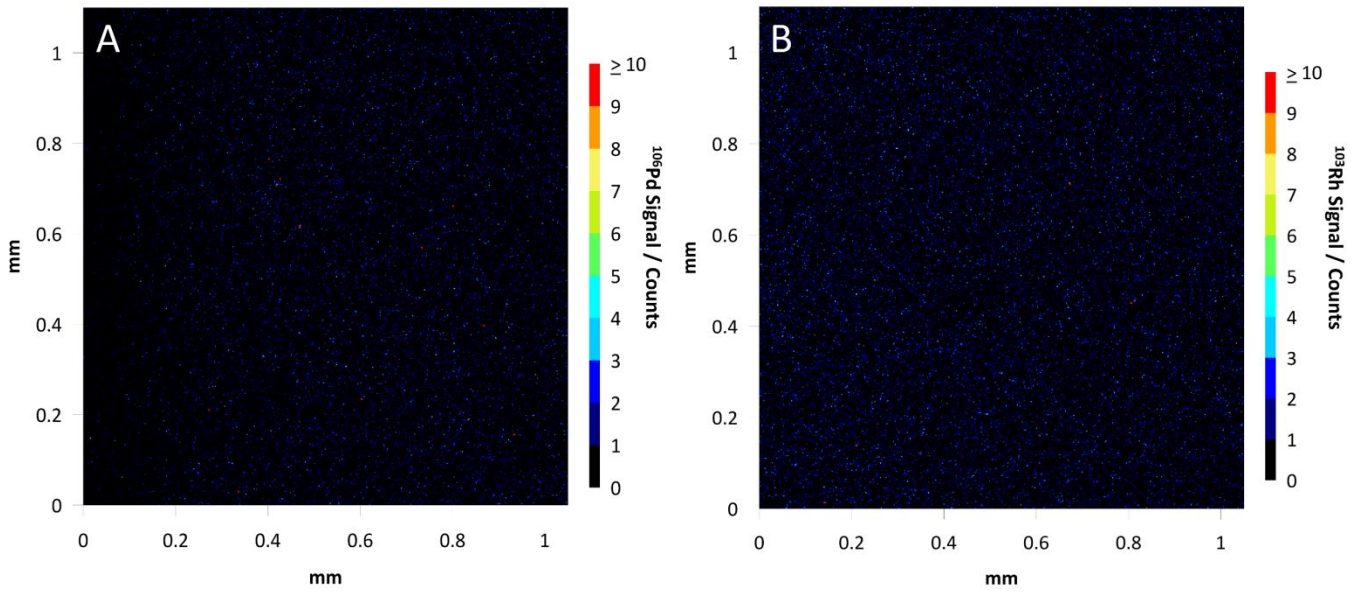

Figure S13. Analysis of Palladium (A) and Rhodium (B) in 0 µM dosed explant control samples.

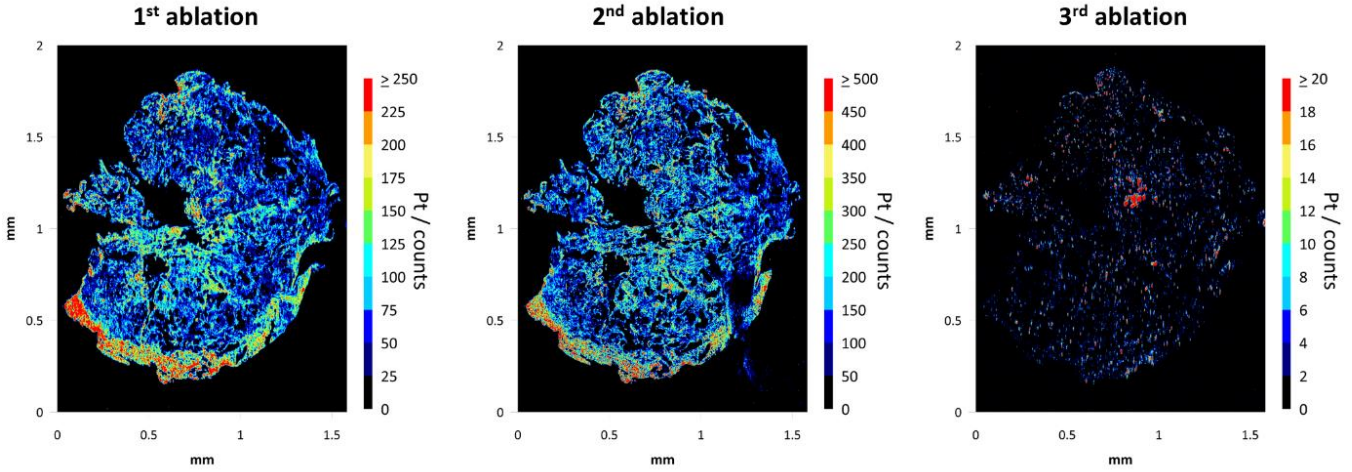

Figure S14. An explant exhibiting varied morphology was ablated layer-by-layer until no tissue remained. Pass 1 and 2 show a similar distribution, with high Pt signal in the top, centre and lower edge of the tissue. By the third pass only minor traces of cisplatin remained.

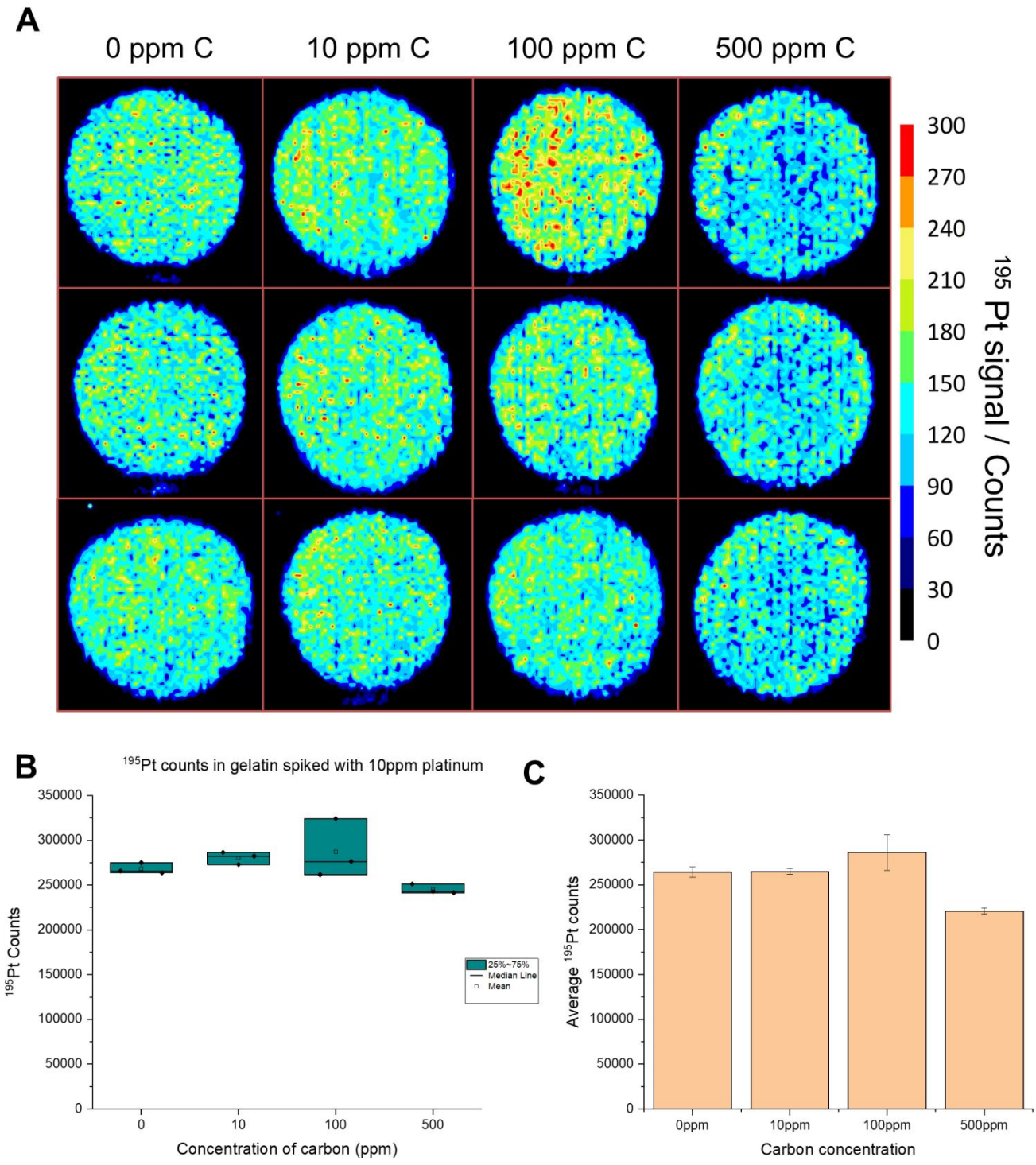

Figure S15. Analysis of platinum in picolitre gelatine droplets containing 10 ppm Pt, with carbon concentrations in the range of 0-500 ppm. Image A shows LA-ICP-MS analysis of the platinum distribution in the droplets. The signals in each droplet were then summed and the average for each of the 3 replicates taken. Images B and C show a box and whisker diagram and a bar chart of the processed data, respectively.

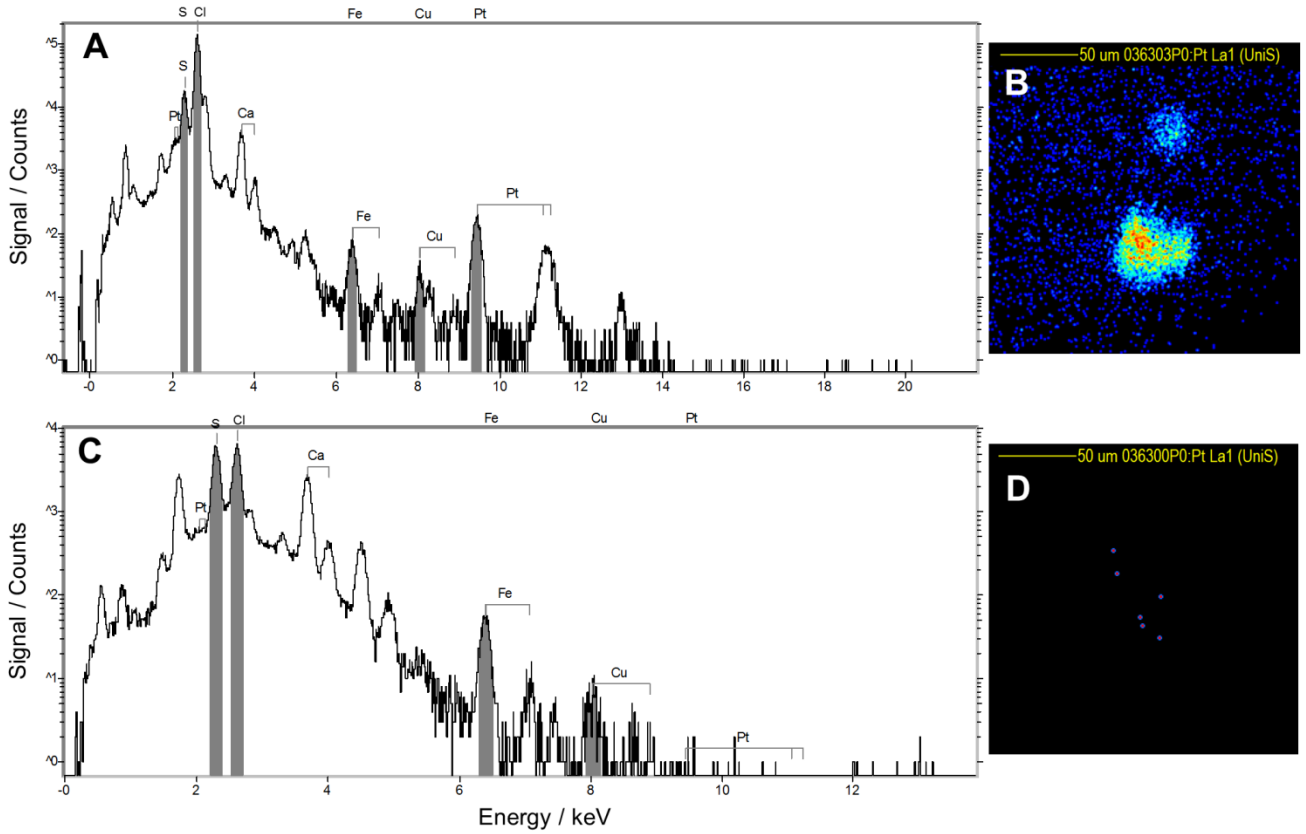

Figure S16. Panels A and B show the PIXE spectrum and PIXE image for the analysis of a region of Pt spiked gelatin containing carbon particulate. This is the same sampled area as shown in the backscattered spectrum in Figure 4D of the paper. Panels C and D show the PIXE spectrum and PIXE image of carbon particulate in a non-spiked sample. The data confirms that carbon particles are associated with a strong Pt signal in the spiked samples, but do not naturally contain platinum.

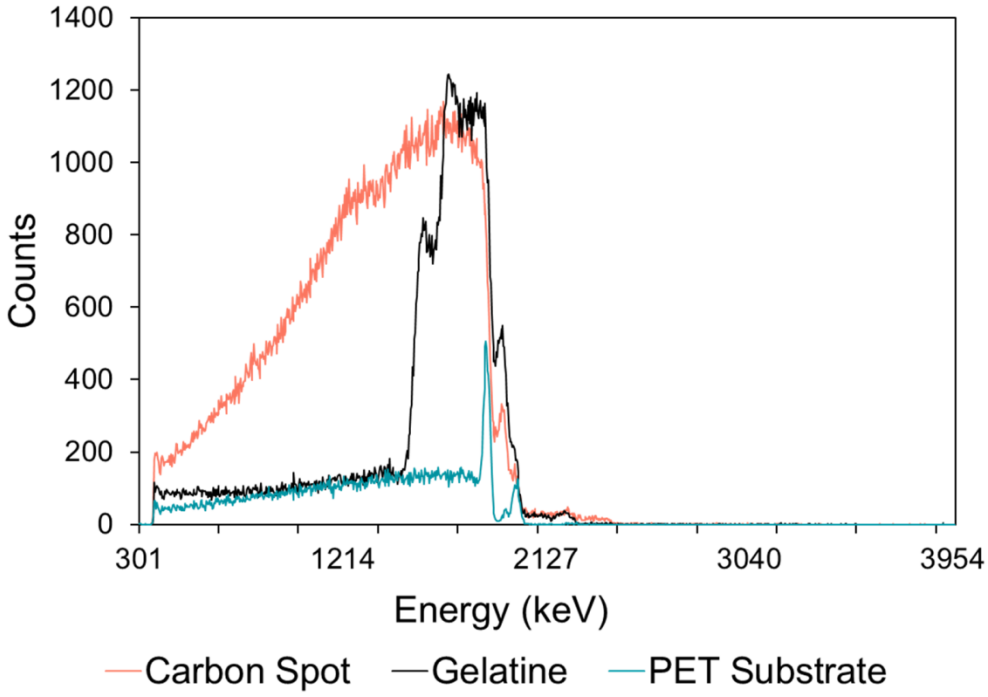

Figure S17. An overlay of the backscattered spectrum extracted from a carbon spot (rose), gelatine only (black) and PET substrate (teal).

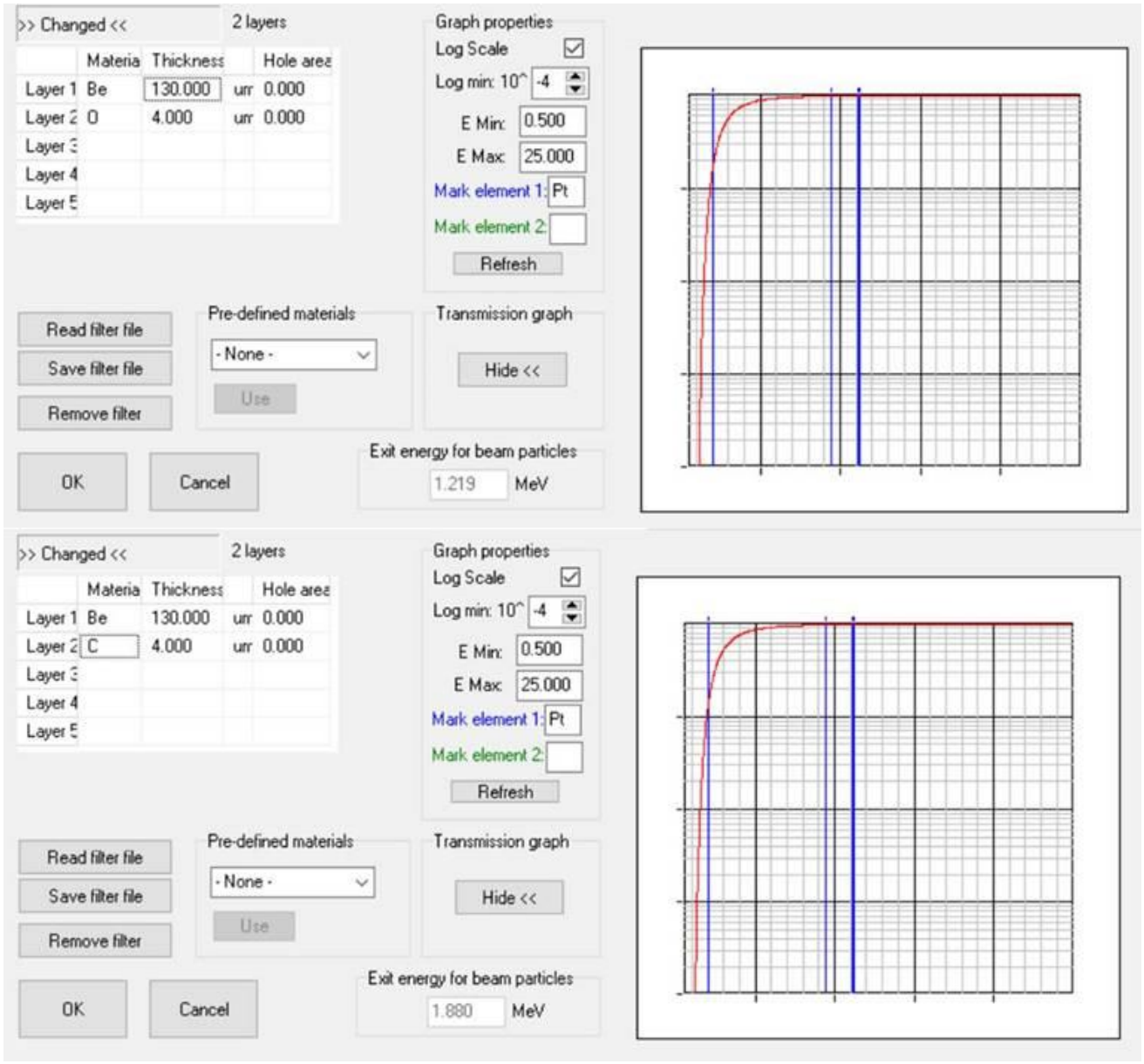

Figure S18. A simulation (using Omdaq) of X-ray transmission through a layer of 4 microns of O (top panel) and C (bottom panel), as well as the usual Be filter. The x axis is x-ray energy, and the y axis is transmitted intensity (logarithmic, with 100% transmission at the top). The blue lines denote the Pt lines, with the Pt L lines (right) showing 100% transmission for either matrix.